

Spotlight Selection | Environmental Microbiology | Full-Length Text

Myxococcus xanthus fruiting body morphology is important for spore recovery after exposure to environmental stress

Dave Lall, Maike M. Glaser, Penelope I. Higgs

AUTHOR AFFILIATION See affiliation list on p. 17.

ABSTRACT Environmental microorganisms have evolved a variety of strategies to survive fluctuations in environmental conditions, including the production of biofilms and differentiation into spores. Myxococcus xanthus are ubiquitous soil bacteria that produce starvation-induced multicellular fruiting bodies filled with environmentally resistant spores (a specialized biofilm). Isolated spores have been shown to be more resistant than vegetative cells to heat, ultraviolet radiation, and desiccation. The evolutionary advantage of producing spores inside fruiting bodies is not clear. Here, we examine a hypothesis that the fruiting body provides additional protection from environmental insults. We developed a high-throughput method to compare the recovery (outgrowth) of distinct cell types (vegetative cells, free spores, and spores within intact fruiting bodies) after exposure to ultraviolet radiation or desiccation. Our data indicate that haystack-shaped fruiting bodies protect spores from extended UV radiation but do not provide additional protection from desiccation. Perturbation of fruiting body morphology strongly impedes recovery from both UV exposure and desiccation. These results hint that the distinctive fruiting bodies produced by different myxobacterial species may have evolved to optimize their persistence in distinct ecological niches.

IMPORTANCE Environmental microorganisms play an important role in the production of greenhouse gases that contribute to changing climate conditions. It is imperative to understand how changing climate conditions feedback to influence environmental microbial communities. The myxobacteria are environmentally ubiquitous social bacteria that influence the local microbial community composition. Defining how these bacteria are affected by environmental insults is a necessary component of predicting climatic feedback effects. When starved, myxobacteria produce multicellular fruiting bodies filled with spores. As spores are resistant to a variety of environmental insults, the evolutionary advantage of building a fruiting body is not clear. Using the model myxobacterium, *Myxococcus xanthus*, we demonstrate that the tall, haystack-shaped fruiting body morphology enables significantly more resistance to UV exposure than the free spores. In contrast, fruiting bodies are slightly detrimental to recovery from extended desiccation, an effect that is strongly exaggerated if fruiting body morphology is perturbed. These results suggest that the variety of fruiting body morphologies observed in the myxobacteria may dictate their relative resistance to changing climate conditions.

KEYWORDS *Myxococcus xanthus*, spore, fruiting body, UV, desiccation

Environmental communities of microorganisms play important roles in biogeochemical cycling, including the production and consumption of greenhouse gases such as carbon dioxide, methane, and nitrous oxide (1, 2). It has become increasingly important to understand how resulting changes to the climate (i.e., increased drought/flooding or changes in UV index as a result of cloud cover or ozone recovery), will impact environmental microbial activities (3, 4).

Editor Jennifer B. Glass, Georgia Institute of Technology, Atlanta, Georgia, USA

Address correspondence to Penelope I. Higgs, pihiggs@wayne.edu.

The authors declare no conflict of interest.

See the funding table on p. 17.

Received 23 August 2024 Accepted 18 September 2024 Published 4 October 2024

Copyright © 2024 American Society for Microbiology. All Rights Reserved.

Downloaded from https://journals.asm.org/journal/aem on 04 March 2025 by 141.217.50.159.

The myxobacteria are a group of highly social predatory or cellulolytic bacteria that are thought to be important for influencing environmental microbial community structure (5–9). Analysis of data from the Earth Microbiome Project determined that the myxobacteria are among the most widely distributed prokaryotic orders on Earth (10). They have been identified in a wide variety of terrestrial and marine environments (11), including some extreme environments, such as the Sahara with a high UV index and long periods of desiccation (12). Thus, understanding how myxobacteria can persist in environments is important to fully understand how microbial communities will be affected by, and consequently contribute to, climate change (3, 4).

Most myxobacteria have the ability to produce dormant spores that display increased resistance to environmental insults such as UV, desiccation, and heat (13). Interestingly, myxobacterial spores are typically produced inside macroscopic fruiting bodies produced at the culminating stage of an elaborate multicellular developmental program (13). Different myxobacterial genera produce distinctive fruiting bodies, with heights in the range of 0.1-1 mm and morphologies ranging from simple mounds containing spores embedded in extracellular matrix (ECM) to elaborate tree-like structures in which spores are housed in rigid, thick-walled sporangioles (13, 14). An attractive early hypothesis is that the spore state enables survival under unfavorable conditions, while the function of fruiting bodies is to keep the spores together to allow group dispersal and/or germination en masse upon return to favorable conditions (13, 15, 16). The latter hypothesis is suggested because most of the myxobacteria uptake nutrients in a process that is likely facilitated by the collective secretion of degradative enzymes to break down external macromolecules. However, additional, but not mutually exclusive, roles for fruiting bodies have also been proposed, including production of higher quality spores by maturation within a fruiting body, attraction of insects to facilitate dispersal, or additional protection from environmental insults (17, 18).

The best characterized of the myxobacteria is *Myxococcus xanthus*. In the vegetative state, cells obtain nutrients from prey microorganisms or decaying organic matter. While single *M. xanthus* cells can kill prey (19–21), it has been argued that group secretion of antibiotics and hydrolytic enzymes facilitates the breakdown of prey and resulting macromolecules for uptake by cells (22–24). Upon nutrient limitation, *M. xanthus* communities form simple haystack-shaped, soft fruiting bodies, each consisting of approximately 10⁵ metabolically quiescent spores embedded in a matrix of exopolysaccharides, proteins, lipids, and eDNA (25–28). Relative to the vegetative cells, *M. xanthus* spores have been shown to have enhanced resistance to UV, desiccation, heat (up to 60°C for 60 min), enzymatic digestion, detergents, and sonic disruption (29–31). These resistance properties fall far short of endospores produced by common environmental Firmicutes (32).

Here, we explore the hypothesis that myxobacterial fruiting bodies provide additional protection to the spores from environmental insults. We first developed a high-throughput method to assay community recovery after exposure to two common environmental insults, UV exposure and desiccation. We used this method to confirm that free spores are more resistant than vegetative mats to UV exposure, but the fruiting body community can recover after at least fourfold longer exposure. Production of small or shallow fruiting (SF) bodies results in significantly reduced recovery after UV exposure. In contrast, relative to the free spores, wild-type (WT) fruiting bodies provide little additional protection to short-term (<1 week) desiccation and hinder recovery from extended (>2 weeks) desiccation. However, the production of shallow fruiting bodies significantly impedes recovery compared to free spores, likely due to severe dehydration of the fruiting body matrix material. These studies have important implications for environmental community composition in the face of more frequent and extreme environmental fluctuations arising from climate change.

MATERIALS AND METHODS

Strains and media

The following *M. xanthus* strains were used in this study: DZ2 (33), PH1054 [DZ2 $\Delta espA$ $\Delta espC$ $\Delta (redCDEF)$ todK::miniTn5 (tet) $\Omega 8846$; here, termed shallow fruiting mutant] (34–37), PH2036 {DZ2 $attB::Pr_{pilA}$ -mCherry [pFM16 (38); Kn^R]}, and PH2037 (PH1054 attB::pFM16). Strains were grown under vegetative conditions in CYE broth [1% casitone, 0.5% yeast extract, 10 mM 3-(N-morpholino) propanesulfonic acid (MOPS) pH 7.6, and 4 mM MgSO₄) (33) on an orbital shaker at 220 rpm and 32°C. Strains were recovered from permanent stocks on CYE agar plates (CYE and 1.5% agar), containing kanamycin at 100 μ g mL⁻¹ as necessary, and grown at 32°C.

Bacterial growth curve measurements

To generate flask culture growth curves, cells were inoculated into 15 mL of CYE broth and grown overnight at 32°C with shaking at 220 rpm. Cells were subcultured 1:100 into 45 mL fresh CYE broth in 500-mL Erlenmeyer flasks and incubated as above. Every 4 hours, 1 mL of culture was withdrawn and absorbance at 550 nm (A_{550}) was recorded in a spectrophotometer (Ultrospec 2100, Amersham Biosciences) using cuvettes with 1 cm pathlength (Table 1: flask growth, spectrophotometer measurement) or by placing 0.2 mL in triplicate wells of a 48-well plate followed by absorption measurement in a Tecan Spark 10M plate reader (Table 1: flask growth, plate reader measurement). Once samples reached $A_{550} > 1$, they were diluted in CYE before absorbance readings.

For growth curve analysis of broth cultures in 48-well plates (CytoOne, USA Scientific), overnight cultures were diluted to an A_{550} of 0.035 in fresh CYE, and 200 μ L was seeded into triplicate wells. Plates were incubated in a Tecan Spark 10M for 72 hours with continuous orbital shaking (216 rpm) at 32°C, and the A_{550} was recorded automatically every 2 hours (Table 1: plate reader growth and measurement). Each growth curve was blanked to the respective initial (T=0) A_{550} reading, such that the initial A_{550} reading is plotted as 0. Final growth curves were plotted as the average and associated standard deviation of A_{550} values recorded from three independent biological replicates, each containing three technical replicates, versus time.

The length of the lag phase was measured as the length of time to reach A_{550} of 0.02, which was determined by solving for time using the slope equation from a trendline generated using three data points surrounding the 0.02 A_{550} value. Doubling times (t_d) were calculated using the equation $t_d = \ln 2/\mu$, where μ is the growth rate. The growth rate was calculated as $\mu = (\ln A_2 - \ln A_1)/(t_2 - t_1)$, where t_1 , t_2 and t_2 , t_2 correspond to values in the exponential growth phase (39). The onset of the stationary phase was taken as the time corresponding to the peak t_2 value recorded.

Generation of cell states

To generate vegetative mats, overnight cultures were diluted to $0.035\,A_{550}$ in fresh CYE, and 200 μ L was seeded in triplicate wells of a 48-well plate (CytoOne, USA Scientific), followed by incubation for 24 hours at 32°C without shaking. Fruiting bodies were generated in submerged culture (40). Briefly, the CYE over-layer was removed from

 TABLE 1
 Growth characteristics of M. xanthus strains grown in 48-well tissue culture plates

Strain		Lag (hours) ^a			Doubling time (hours)			Peak A ₅₅₀			Onset stationary phase (hours)		
Growth ^b		Flask	PR^d		Flask	PR^d		Flask	PR^d	_	Flask	PR^d	
A ₅₅₀ ^c	S	PR	PR	S	PR	PR	S	PR	PR	S	PR	PR	
WT	5.7	14.2	11.1	5.3	4.6	8.7	6.0	1.0	0.6	48	56	44	
SF	5.1	11.0	11.4	6.3	4.6	7.7	6.7	1.0	0.7	48	56	40	

^aSee Fig. S1C for increased resolution of the lag times observed for the WT.

^bCells were grown in a flask with shaking at 220 rpm or plate reader (PR) in 48-well plate at 216 orbital rpm.

^{&#}x27;Recorded by spectrophotometer (S), where the culture was diluted to <1 A₅₅₀ in fresh media where necessary or by PR without dilution.

^dExperimental set-up used for subsequent outgrowth analyses.

vegetative mats, replaced with 200 µL of sterile MMC starvation media (10 mM MOPS, pH 7.6, 2 mM CaCl₂, and 4 mM MgSO₄), and further incubated at 32°C without shaking for 120 hours.

To generate free spores, submerged cultures were generated in 100 mm Petri dishes as above, except 16 mL volumes were used. Five days post-starvation, fruiting bodies were harvested, pelleted $(4,600 \times q, 10 \text{ min, RT})$, resuspended in 0.5 mL sterile water, and spores were dispersed by mild sonication at output 10%, 0.5 second on/0.5 second off for a total of 23 seconds (Branson Sonifer 250). For half sonication controls, spores were dispersed at output 10%, 0.5 second on/0.5 second off for a total of 10 seconds. Spores were diluted ~30-fold in sterile water, and 200 µL volumes were added to triplicate wells of a 48-well plate using low-binding pipette tips (Sorenson) to minimize sticking of spores and fruiting bodies during pipetting. Spores were allowed to settle onto the surface of the well for 60 min at RT.

To generate chemically induced quick spores (41), overnight cultures of strains were sub-cultured 1:10 and grown for at least two doublings to an A_{550} of 0.2–0.35. Ten molar sterile glycerol was added to the cultures to a final concentration of 0.5 M, and cultures were incubated at 32°C in an orbital shaker at 220 rpm for 24 hours to produce fully mature quick spores. Cultures were pelleted (4,600 \times g, 20 min, RT), resuspended in 0.5 mL sterile water, and gently dispersed as described for free spores. Spores were enumerated in a counting chamber, and 4×10^6 spores in 50 µL were added to each well.

For outgrowth analysis of the vegetative mats, fruiting bodies, or free spores, samples were generated in triplicate wells in a 48-well plate, the respective overlay media were replaced with 200 µL fresh CYE, and plates were incubated in the plate reader with continuous orbital shaking (216 rpm) at 32°C for 72 hours. A₅₅₀ values were automatically recorded every 2 hours. CYE media served as the blank. Growth curves were plotted as described above. The final outgrowth curves were calculated as the average and associated standard deviation of growth curves generated from three independent biological replicates, each containing triplicate technical replicates. Wells in which condensation on the lid obscured necessary readings were not included.

Alteration of wild-type fruiting body size by surface heterogeneity

Randomly distributed 10 µm Non-Functionalized Colloidal Silica Nanospheres (ALPHA Nanotech) were sterilized as follows: 1 mL of 1 mg/mL beads were pelleted 4,600 imesq for 10 min at RT and resuspended in 1 mL of 70% (vol/vol) ethanol followed by incubation for 15 min with intermittent agitation. The beads were pelleted and the ethanol incubation was repeated. Beads were then treated two times with 1 mL of sterile water as described above and then serially diluted twofold in sterile water. Final bead concentrations were determined in a Helber cell counting chamber (Hawksley, UK).

Overnight cultures of the wild-type strain were diluted to 0.035 A_{550} in fresh 2× CYE. Next, 100 µL of diluted culture and 100 µL of nanobead dilutions (or water) were mixed and then seeded in triplicate wells of a 48-well plate. Fruiting bodies were induced as indicated above. Spores produced were ascertained by harvesting triplicate wells, and heat- and sonication-resistant spores were enumerated (40). Spores could be easily distinguished from beads based on size. Exposure to UV and bacterial growth curve measurements were performed as described below, except the optical density from wells containing equivalent bead concentrations without cells was subtracted from the outgrowth cultures.

UV stress assay

Vegetative mats, fruiting bodies, or free spores were generated in 48-well plates as described above, with one plate used per cell state. The wild type and SF mutant were added to 21 wells each; three wells served as cell-free blanks. Overlay media from all wells were replaced with 50 µL of sterile water (such that all cell states were exposed to UV in the same relative conditions), and triplicate wells for each strain were exposed to 0, 1, 2, 4, 8, 16, or 32 min of 306 nm UV supplied by an inverted transilluminator rated

October 2024 Volume 90 Issue 10

at 8,000 μ W/cm² (Model FB-TI-88A, Fisher Scientific, USA) that was placed 10 cm above the uncovered plate. Aluminum foil was used to shield the remaining wells. Following UV exposure, an additional 50 μ L sterile water and 100 μ L of fresh 2× CYE were added to each well, and outgrowth was measured in a plate reader as described above.

To test whether manipulation of fruiting bodies leads to increased UV sensitivity, wild-type fruiting bodies were developed in 100 mm Petri dishes as above. Five days post-starvation, fruiting bodies were harvested and pelleted as above and resuspended in 0.5 mL sterile water by pipetting vigorously 30 times using a low-binding pipette tip. In total, 200 μL volumes were added to triplicate wells of a 48-well plate. Fruiting bodies were allowed to settle onto the surface of the well for 60 min at RT; the water was removed and then replaced with 50 μL of sterile water. UV exposure and outgrowth were performed as described above.

Desiccation assay

For desiccation of vegetative mats, wild-type and SF mutant strains were each seeded in three wells (48-well plate), and the plate was incubated at 32°C without shaking. This process was repeated 16, 24, 28, 30, 31, and 32 days later. Twenty-four hours after the respective seeding times, CYE media were removed, and the plates were incubated at 32°C. Thus, triplicate wells of each strain experienced 32, 16, 8, 4, 2, 1, or 0 days of desiccation. Thirty-three days after the initial seeding, 200 µL of fresh CYE was added to all wells to induce outgrowth. Three wells served as cell-free blanks. Outgrowth was measured in a plate reader as described above. Desiccation of fruiting bodies and free spores followed the same process, except that fruiting bodies and free spores were generated by seeding vegetative cells 6 days in advance of the respective desiccation start times, and starvation was induced 24 hours later. Free spores were obtained from fruiting bodies generated in 100 mm Petri dishes and processed as described above.

Determination of time to recover after insult

Recovery curves were plotted as described for the growth curves above. Final recovery curves were plotted as the average A_{550} and associated standard deviation from three independent biological replicates, each containing three technical replicates, versus time. We note that extended outgrowth incubation times (\gtrsim 36 hours) sometimes resulted in increased variability in A_{550} measurements primarily due to the buildup of condensation on the lid affecting A_{550} readings.

An A_{550} of 0.2 was selected as a reference indicating early exponential growth. Recovery time was calculated using the slope equation from a trendline derived from four data points surrounding $A_{550} = 0.2$. The relative fold recovery for each cell state was expressed as treated recovery time (t_T) /untreated recovery time (t_{UT}) . The maximal observable relative recovery (MORR) for each assay was calculated as 72 hours divided by the average time recovery time for each untreated cell state. The MORR for each cell state was depicted for each condition. Cultures that did not recover within 72 hours were plotted at the MORR line and represent values greater than or equal to that value. Statistical significance of relative recovery times was determined either by two-way ANOVA followed by Tukey's multiple comparison test or by t-test, as indicated in each figure. Values at the MORR were only considered for statistical significance if they were compared against values below the MORR line. Graphs and statistical analyses were generated in GraphPad Prism (version 10.3.0). Figures were generated in Affinity Designer (1.10.8).

Imaging of fruiting bodies, vegetative mats, and free spores

To image vegetative mats, fruiting bodies, and desiccated fruiting bodies, the respective cell states were generated in " μ -Dishes ^{35 mm, high}" confocal dishes (ibidi Technologies; hereafter, ibidi dishes) using 2.1 mL volumes of seed cultures or starvation buffer. Images were captured using a Leica M80 stereomicroscope and a Leica DMC2900 camera (50×

October 2024 Volume 90 Issue 10

magnification), or a Zeiss Axio Imager, M1 microscope, and Cascade 1K camera (100–1,000 \times magnifications). Free spores were generated as described above, and 10 μ L aliquots were spotted onto agar pads (42).

For confocal imaging of wild-type and SF mutant fruiting bodies, strains PH2036 and PH2037 (expressing mCherry from the constitutive pilA promoter in DZ2 and PH1054 backgrounds, respectively) were developed in ibidi dishes for 48 hours. Fruiting bodies were imaged using a Leica TCS SP8 inverted confocal microscope. mCherry fluorescence was detected using a 552-nm wavelength laser (5% power) for excitation, a 585–630 nm emission spectra, and a gain of 750 V. Fruiting bodies were imaged from the base to the top with a step size of 1 μ m and a line average of 4 at 1,024 × 1,024 resolution.

To determine the heights of fruiting bodies, wild-type (DZ2) and SF mutant (PH1054) strains were induced to develop in ibidi dishes for 5 days. Fruiting bodies were stained in MMC supplemented with 2 mM MnCl $_2$ and 15 μ L of Fluorescein-conjugated Concanavalin A (5 mg/mL; solubilized in 0.1 M NaHCO $_3$ pH 8.3, Karlsruhe, Germany) and incubated for 30 min at RT in the dark. The stain was removed, and fruiting bodies were washed twice with 1 mL MMC and 2 mM MnCl $_2$. For microscopy, 2 mL of MMC was added back to the cells. The fluorescein signal was detected using a 552-nm wavelength laser (15% power) for excitation, a 494–572-nm emission spectra with an inverted TCS-SP5 confocal microscope (Leica, Bensheim, Germany). Fruiting bodies were imaged from the base to the top with a step size of ~0.9 μ m. Image data and fruiting body heights were processed by using IMARIS software package (Bitplane AG, Zurich, Switzerland) or Volocity Software (Perkin Elmer).

RESULTS

Growth characteristics of M. xanthus cultivated in 48-well plates

We first set out to generate a high-throughput method to monitor the growth of *M. xanthus* wild-type strain DZ2 using a plate reader to measure growth in 48-well plates. To understand how variables, such as aeration, inability to dilute samples of dense cultures, and absorbance pathlength, affected the apparent growth characteristics, we compared data obtained from the growth of the wild-type strain under standard broth culture conditions to that obtained by the plate reader. *M. xanthus* growth and measurement in standard conditions produced a reproducible growth curve with distinct lag, log, stationary, and death phases (Fig. S1). The wild-type doubling time was calculated as 5.3 hours and peak cell density was measured at 6.0 *A*₅₅₀ (Table 1).

When the absorbance of the flask cultures was instead measured undiluted in a plate reader, the overall apparent A_{550} was reduced (Fig. S1B), likely because the pathlength of the absorbance measurement is 0.26 cm compared to 1 cm in the spectrophotometer. Analysis of these data led to aberrations in the calculated doubling time, lag time, and onset of stationary phase (Table 1). This may be because the plate reader is less sensitive in reading dilute cultures, and at higher cell densities, the correlation between absorbance and cell number is outside of the dynamic range.

With these parameters established, we next ascertained how culturing *M. xanthus* in 48-well plates affected growth characteristics. We observed that growth of the wild type in wells shortened the lag phase by approximately 3 hours and increased the doubling time by approximately 4 hours (Fig. S1B; Table 1). Furthermore, growth in wells resulted in an apparent onset of the saturation phase 12 hours earlier than observed for growth in flasks, and a death phase could be observed within the 72 hours for which data were collected (Fig. S1B; Table 1). These results suggest that cells cultured in wells may be limited by oxygen and/or nutrient availability compared to those growing in flasks.

Relative outgrowth of *M. xanthus* vegetative mats, free spores, and fruiting bodies

We next took advantage of the plate reader to determine the relative outgrowth of the distinct cell states: vegetative mats, fruiting bodies, or free spores dispersed from

October 2024 Volume 90 Issue 10

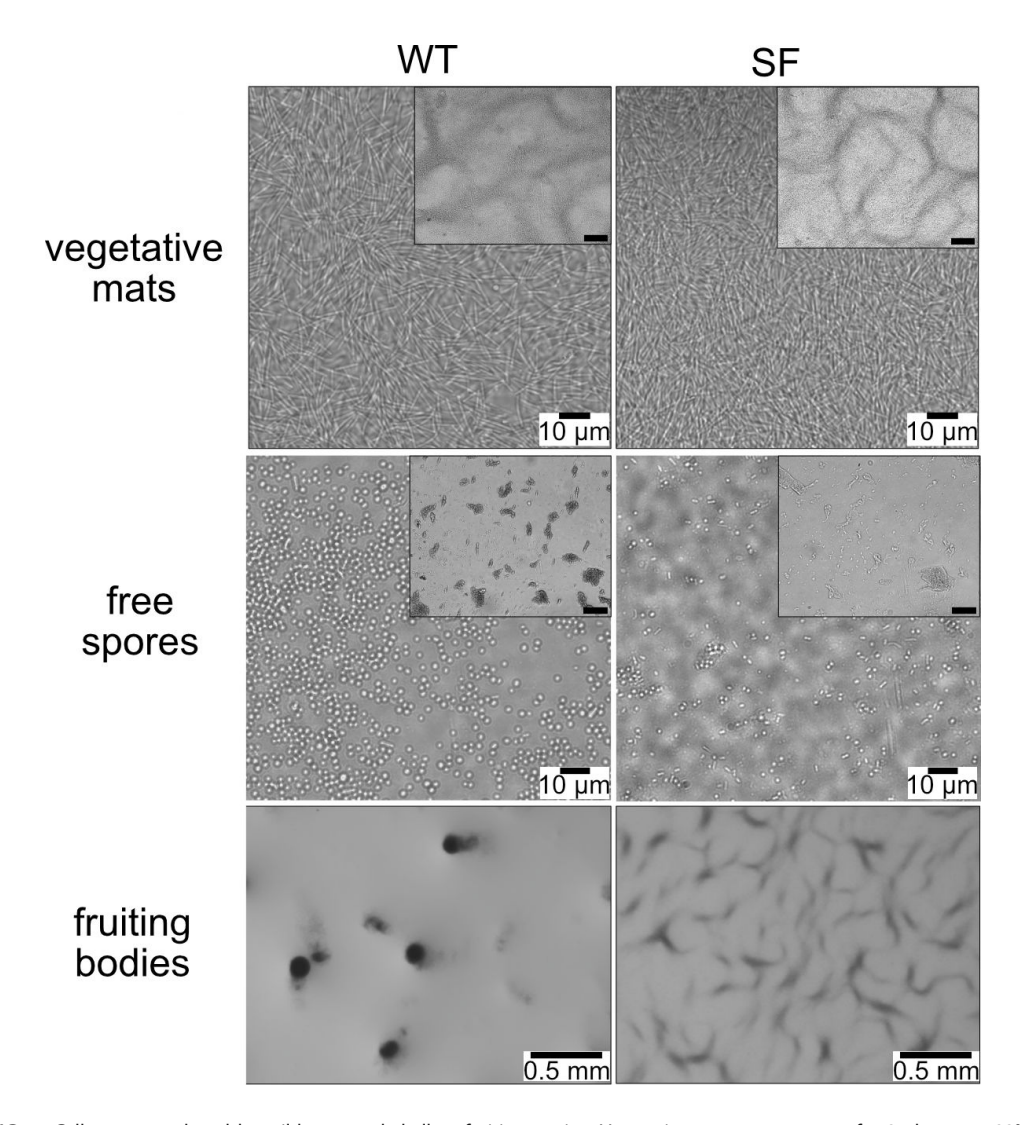


FIG 1 Cell states produced by wild-type and shallow fruiting strains. Vegetative mats were grown for 24 hours at 32°C, free spores were released from fruiting bodies with mild sonication, and fruiting bodies were induced to develop under submerged culture for 120 hours. Scale bars represent 100 µm unless otherwise indicated.

fruiting bodies (Fig. 1). To monitor the outgrowth of each state, the respective overlay was replaced by fresh nutrient-rich broth, and the plates were incubated in the plate reader using the incubation parameters defined above. We observed that vegetative mats experienced a lag phase of 5.5 ± 0.8 hours, compared to 14 ± 2 and 24 ± 1 for mature fruiting bodies and free spores, respectively (Fig. 2). The longer lag phase observed by fruiting bodies and free spores reflects the requirement for these cell states to first germinate. Additionally, however, each cell state contains different numbers of initial cells/spores, because approximately 80% of cells lyse during development and not all spores are viable (43). Cell counting techniques that determined the number of vegetative cells, spores, or peripheral rods produced per unit area under our developmental conditions (43) were employed to estimate that at the beginning of outgrowth, vegetative mats contain $\sim 5 \times 10^7$ cells per well, whereas the fruiting bodies contained 6.5×10^6 spores and were estimated to contain $\sim 2 \times 10^6$ peripheral rods per well. We determined that free spores were present at approximately 4×10^6 spores per well.

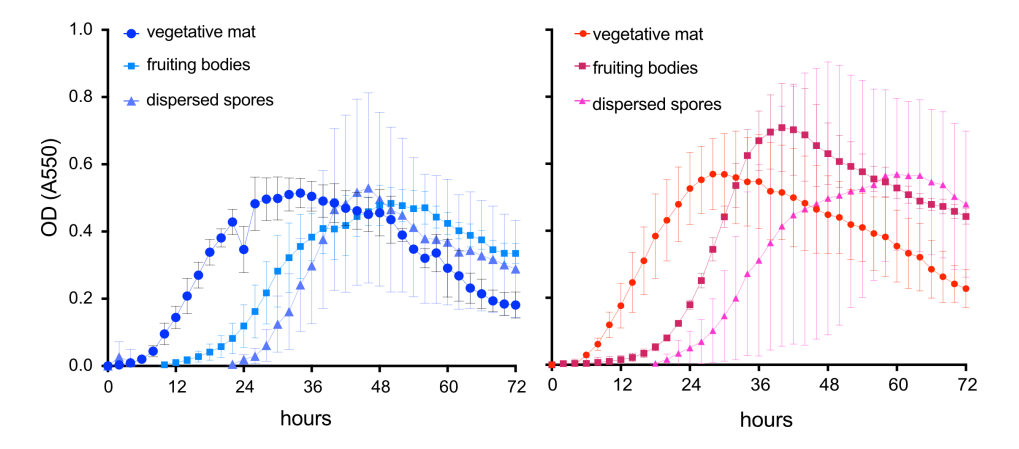


FIG 2 Outgrowth of cell states in the wild-type (left, blue shades) and shallow fruiting mutant (right, red shades) strains. Vegetative mats (circles), fruiting bodies (squares), and dispersed spores (triangles) were generated in 48-well plates. To induce outgrowth, rich medium was added (0 hours), cells were incubated at 32° C with shaking in a plate reader, and A_{550} was recorded every 2 hours for 72 hours. Data points are the average and associated standard deviation of three independent biological replicates, each containing three technical replicates.

Assembly of spores into fruiting bodies provided additional protection against UV stress

Having established the outgrowth characteristics of each cell state, we next examined the relative outgrowth rates after exposure to UV. For these experiments, triplicate wells of vegetative mats, free spores, or intact fruiting bodies were exposed to 0, 1, 2, 4, 8, 16, and 32 min of UV at 306 nm (0.08 KJ/m²/second). Outgrowth was then induced and monitored as described above. Analysis of three independent biological replicates indicated the time to recover to the early log phase corresponded to increasing length of UV exposure (Fig. S2), suggesting that the relative recovery period reproducibly corresponded to the fraction of the community surviving UV exposure. Furthermore, the relative recovery pattern was also observed if cells were instead harvested, serially diluted, and directly spotted on rich media agar plates (Fig. S3A). Together, these data suggest that relative recovery time was useful as a way to generate quantitative data on the relative tolerance to insult exposure.

To compare the relative ability of the distinct cell states to withstand UV exposure, we ascertained the time for each exposed culture to reach the early log phase (apparent $A_{550} = 0.2$). These recovery times were then normalized to the time required for the untreated sample (0 min UV exposure) to reach 0.2 A₅₅₀. The resulting relative recovery times were plotted against minutes of UV exposure for each cell state (Fig. 3). Because of the difference in recovery times for each cell state (Fig. 2), the MORR that could be detected within the 72-hour outgrowth time was depicted on each graph, and any cultures that did not recover by the end of the assay were plotted at the MORR line; these data points represent values greater than or equal to the MORR value. For the wild-type vegetative mats, 1 min of UV exposure resulted in an average threefold increase in time for the community to reach 0.2 A₅₅₀ (Fig. 3). No outgrowth was detected after exposure to 2, 4, or 8 min of UV, suggesting they required at least 5.1-fold more time to recover than the untreated. Analysis of the free spore community suggested that after 1-min UV exposure, spores required only a 1.5-fold relative recovery time. Thus, spores provide some protection from UV irradiation, as has been previously demonstrated (29, 31). However, we did not detect recovery of free spores after 2 min or more of UV exposure (Fig. 3), indicating they required at least 2.2-fold relative recovery. In contrast, recovery of the fruiting body cell state was readily observed, requiring only an average of at least 2.4-fold longer recovery time than the untreated sample even after 8 min of UV exposure. No recovery (within 72 hours) was detected for any cell state after 16 and 32 min of UV exposure (data not shown).

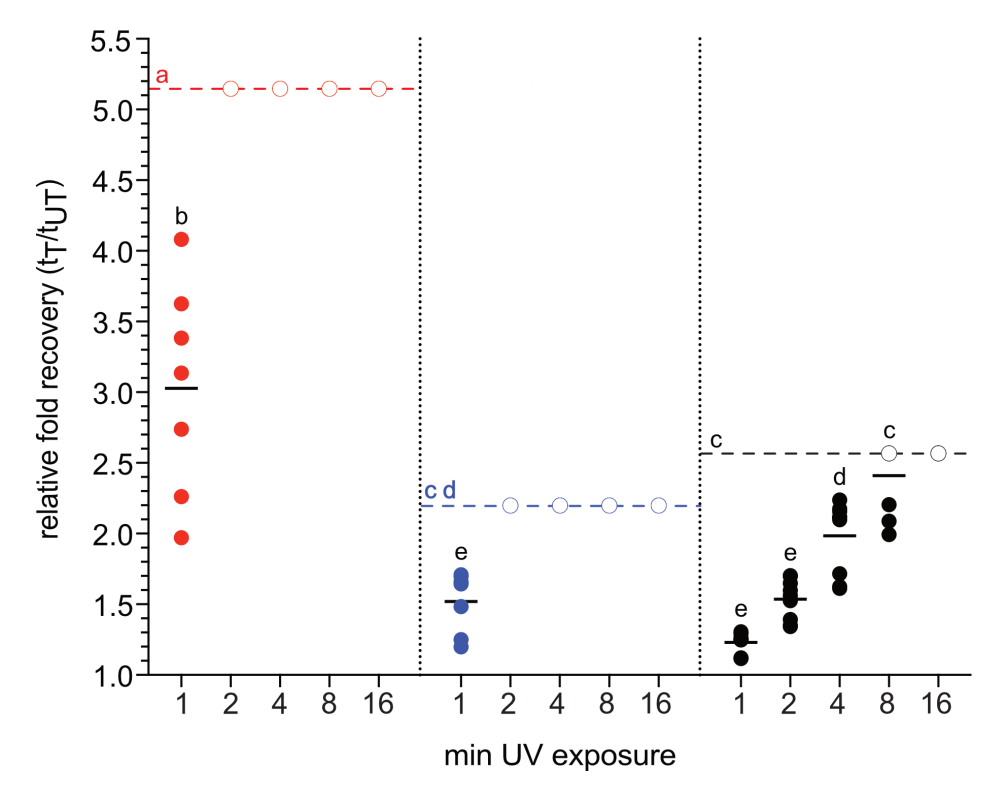


FIG 3 Wild-type fruiting bodies provide significant protection from UV exposure. Relative fold recovery of wild-type vegetative cells (red), free spores (blue), or fruiting bodies (black) after the indicated minutes of UV exposure. Data points are treated samples (t_{T}) normalized to the untreated sample (t_{UT}). t_{T} and t_{UT} are the recovery times necessary for the treated and untreated cultures, respectively, to obtain an A_{550} of 0.2. Horizontal colored dashed lines represent the maximum observable relative recovery that could be detected in 72 hours. Data points (hollow circles) on these lines are greater than or equal to the indicated value. Data were obtained from three independent biological replicates, each containing triplicate samples. Mean is indicated by a short solid line. Statistical significance was determined by performing two-way ANOVA followed by Tukey's multiple comparison test and depicted by a compact letter display. Groups with means that are not statistically significant share the same letter. Colored letters represent a significance group if the maximum observable relative recovery value was used in ANOVA tests.

Control experiments indicated that fruiting bodies that were harvested, resuspended in water, and reseeded prior to at least 2 min of UV exposure displayed no significant differences in recovery from the *in situ*-exposed fruiting bodies (Fig. S4A). Likewise, the generation of free spores using half of the sonication treatment did not increase the free spore recovery (Fig. S4B). Together, these results strongly suggest that manipulation of the fruiting bodies or mild sonication of the free spores was not a significant factor in their increased sensitivity to UV. Thus, these results indicated that while spores do provide protection over vegetative cell mats to shorter intervals of UV exposure, the fruiting body state provides much more protection to extended UV exposure, likely because UV may not effectively penetrate the interior of the fruiting body.

Sporulation is sufficient for efficient recovery from desiccation

We next set out to examine the relative recovery of the cell states after exposure to increasing periods of desiccation. For this assay, vegetative mats, free spores, or fruiting bodies were desiccated for 1, 2, 4, 8, 16, or 32 days at 32°C, and recovery was monitored as described previously. Independent biological replicates demonstrated similar recovery patterns, indicating that recovery time was consistent with the fraction of the population that survived desiccation (data not shown).

We observed that vegetative mats required at least a 6.2-fold relative recovery time after only 1 day of desiccation, but free spores displayed no significant loss of relative recovery for up to 8 days of desiccation (Fig. 4). Prolonged desiccation for 16 and 32 days only increased the recovery time relative to the untreated spores up to an average of 1.7-fold (Fig. 4). Fruiting bodies also provided full protection for at least 4 days of desiccation. Surprisingly, however, after 16 or 32 days of desiccation, fruiting bodies took significantly longer to recover from desiccation than the free spores. Together, these results suggested that sporulation is sufficient to protect cells from desiccation and that assembly of spores into fruiting bodies does not provide additional protection; fruiting bodies may even be slightly detrimental after prolonged desiccation.

Fruiting body morphology influences recovery from environmental insults

To examine whether fruiting body morphology is important for relative recovery from insults, we took advantage of an SF mutant. The SF mutant lacks four genes encoding signaling systems that appear to independently inhibit the accumulation of MrpC, a major transcription factor essential for inducing aggregation into fruiting bodies and sporulation (34, 37, 44, 45). Thus, in the absence of these signaling proteins, MrpC accumulates rapidly, leading to sporulation before the cells have finished moving into aggregation centers likely producing a pseudo-bypass of fruiting body formation (37). As a result, the shallow and misshaped fruiting bodies were $26 \pm 5 \,\mu m$ in height compared to $77 \pm 14 \,\mu m$ in the wild type (Fig. 1 and 5). The spores are viable and resistant to heat at 50° C for 60 min and sonication (37), but for unknown reasons, they appear less phase

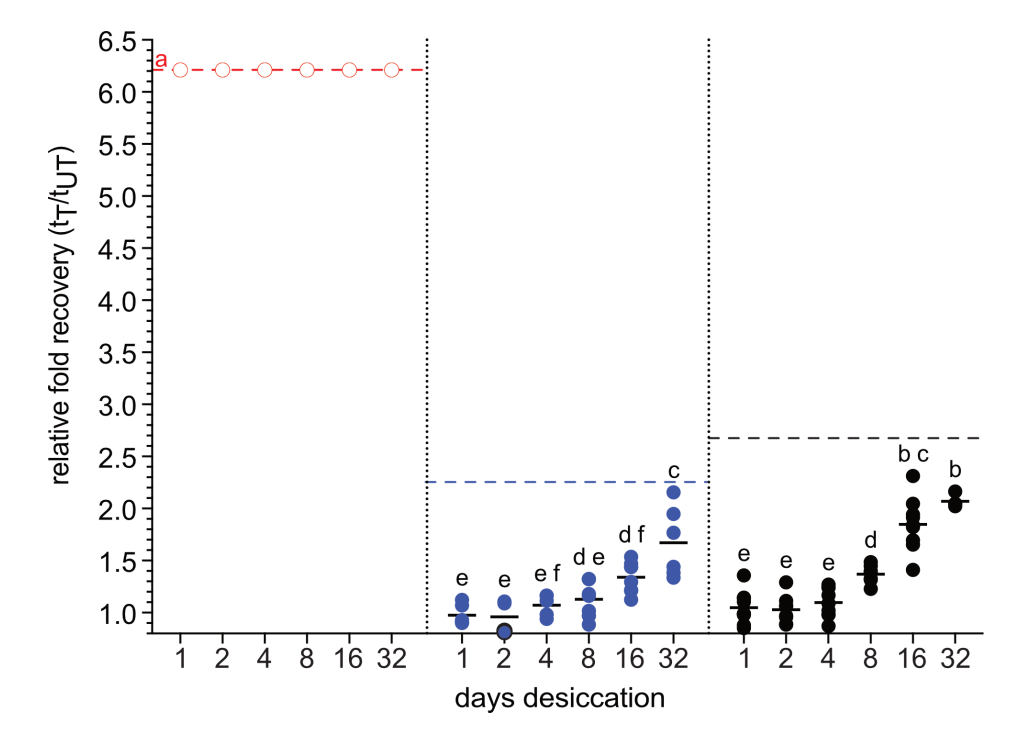


FIG 4 Production of spores is sufficient for protection against desiccation. Relative fold recovery of wild-type vegetative cells (red), free spores (blue), or fruiting bodies (black) after the indicated days of desiccation at 32°C. Data points are treated samples (t_T) normalized to the untreated sample (t_{UT}). t_T and t_{UT} are the recovery times necessary for the treated and untreated cultures, respectively, to obtain an A_{550} of 0.2. Horizontal colored lines represent the maximum observable relative recovery that could be detected in 72 hours. Open circle data points on these lines are greater than or equal to the indicated value. Data were obtained from three independent biological replicates, each containing triplicate samples. Mean is indicated by a short solid line. Statistical significance was determined by performing two-way ANOVA followed by Tukey's multiple comparison test and depicted by a compact letter display. Groups with means that are not statistically significant share the same letter. Colored letters represent a significance group if the maximum observable relative recovery value was used in ANOVA tests.

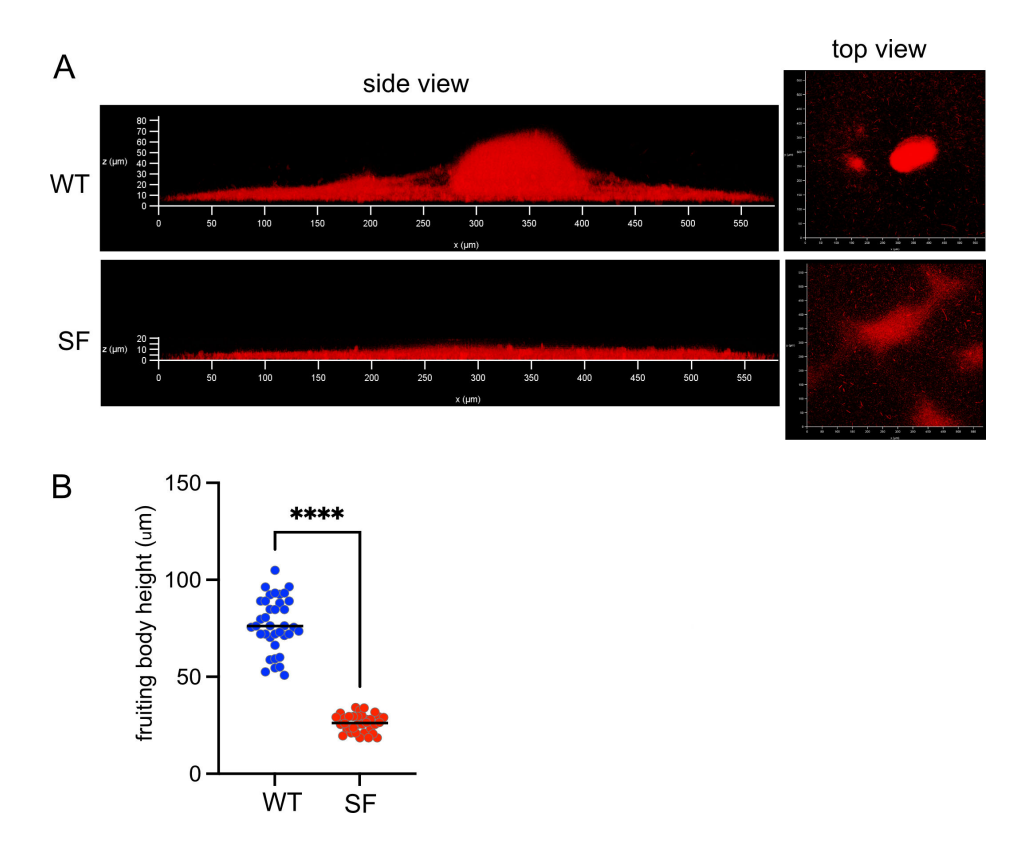


FIG 5 The shallow-fruiting mutant produces shallow and disorganized fruiting bodies. (A) Fluorescence microscopy of wild-type and shallow-fruiting strains expressing the fluorescent protein mCherry driven by the pilA promoter. Strains were developed under submerged culture for 48 hours to form fruiting bodies. (B) Heights of wild-type (blue) and SF mutant (red) fruiting bodies developed under submerged culture for 5 days and stained with FITC-Concanavalin A. WT, n = 37; SF, n = 34 from two independent biological replicates. Statistical significance was determined by an unpaired t-test; *****P < 0.0001.

bright (Fig. 1). To define any possible pleiotropic effects on the mutant spore sensitivity, we first compared the relative sensitivity of 24-hour-induced chemical spores in the wild type and SF mutant. Chemical induction of spores bypasses fruiting body production and directly launches the core sporulation program (38, 41). There was no significant gain in recovery time in the SF mutant spores compared to the wild-type spores with respect to UV resistance or desiccation (Fig. S5). Thus, the SF mutant is a useful tool to assay whether fruiting body morphology is important for extra protection from insults.

Analysis of the vegetative growth pattern of the SF mutant compared to the wild type indicated that it had a similar lag time, the doubling time was reduced by 1 hour, the onset of the stationary phase was approximately 4 hours earlier, and the death phase was not as pronounced (Table 1; Fig. S1A and C). With respect to the outgrowth of the cell states, similar lag times were observed for the vegetative mat, fruiting body, and free spore states of the SF mutant compared to the wild type, respectively (Fig. 2).

Upon exposure to UV, we did not observe any significant differences in relative recovery times of vegetative mats or free spores between the wild type and SF mutant (Fig. 6A; Fig. S3). However, the SF mutant fruiting bodies took significantly longer (*P* < 0.0001) than the wild-type fruiting bodies to recover after 1 min of UV exposure. Recovery after 2 min or more of UV exposure required at least 2.9-fold longer than the untreated state, whereas the wild-type fruiting bodies recovered from up to 8 min of UV exposure with only an average of ~2.4-fold increase in their relative recovery time (Fig. 6A).

As an additional confirmation that fruiting body size is important for recovery after UV exposure, we capitalized on the interesting observation that fruiting body size is affected by surface topology, which can be artificially manipulated by the addition of different

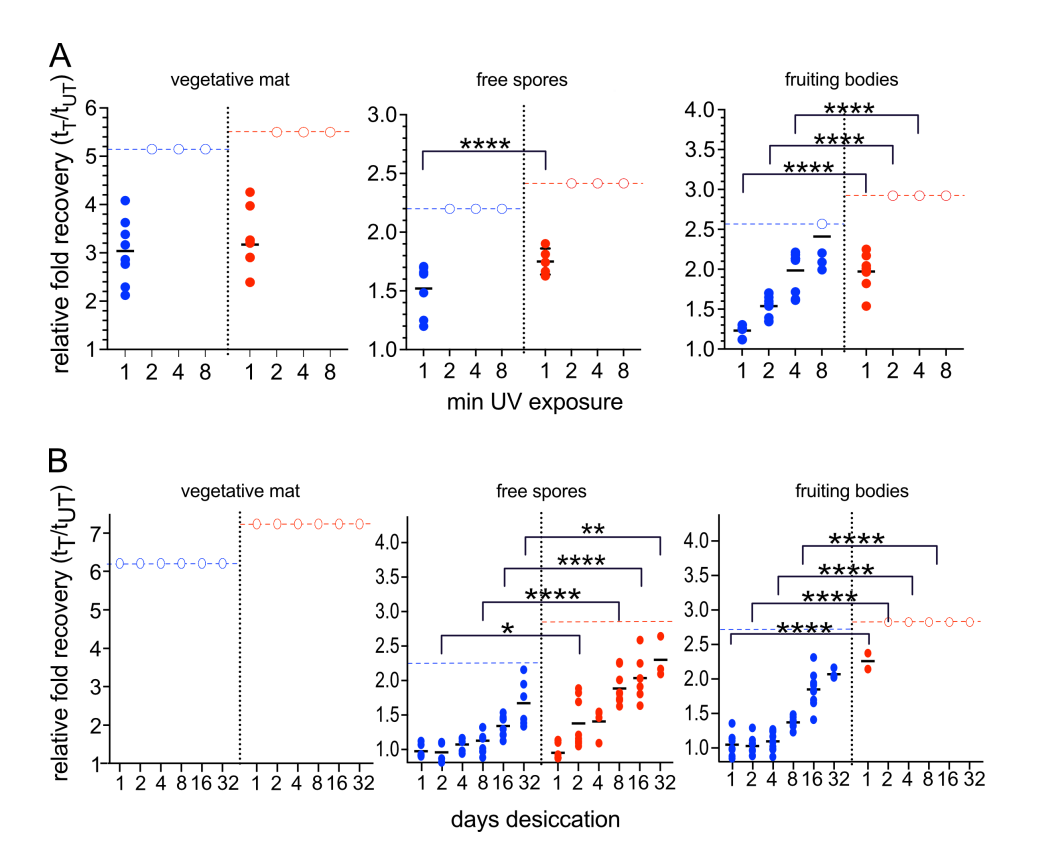


FIG 6 Fruiting body morphology is important for recovery from environmental insults. Relative fold recovery of shallow-fruiting (red) vegetative cells, free spores, or fruiting bodies after UV exposure (A) or desiccation (B) compared to the wild-type data from Fig. 3 and 4, respectively. Data points are treated samples (t_T) normalized to the untreated sample (t_{UT}) . t_T and t_{UT} are the recovery times necessary for the treated and untreated cultures, respectively, to obtain an A_{550} of 0.2. Horizontal colored lines represent the maximum observable relative recovery that could be detected in 72 hours. Open circle data points on these lines are greater than or equal to the indicated value. Data were obtained from three independent biological replicates, each containing triplicate samples. Mean is indicated by a short solid line. Statistical significance was determined by t-test comparing WT vs SF for each time point; where necessary, the Mann-Whitney correction was applied. *P < 0.05; **P < 0.01; ***P < 0.001; and ****P < 0.0001; # would be considered significantly different from the respective WT sample if the maximum observable relative recovery value was used to calculate significance.

concentrations of silica beads (46). We, therefore, adapted this assay to the DZ2 wild-type strain in our submerged culture conditions. As per the observations from Ramos et al. (46), our wild type produced smaller, more numerous fruiting bodies or even microscopic fruiting bodies if they were developed in the presence of 5.2 (\pm 0.95) \times 10⁶ or 17 (\pm 1.7) \times 10⁶ beads/cm², respectively (Fig. 7A and B). Importantly, a similar number of spores could be recovered from cells incubated in the absence or presence of beads (Fig. 7C). After exposure to UV in our assay, the smaller or microscopic fruiting bodies took significantly longer than the standard fruiting bodies to recover from 2 or 4 min of UV exposure (Fig. 7D).

The relative fold recovery times for small or micro-fruiting bodies were not as drastically increased as observed for the SF mutant. For example, 2 min of UV exposure produced an average 2.6-fold increased recovery time for the micro-fruiting bodies (Fig. 7D), whereas the SF mutant fruiting bodies required at least a 2.9-fold increased recovery time (Fig. 6A). However, it was not possible to account for UV shadowing (47) by the beads, suggesting that the exposure recovery times observed in the presence of beads were an underestimation of the full UV effect. Together, our results strongly suggest that a taller, more organized fruiting body structure is required to provide significant protection against UV insults.

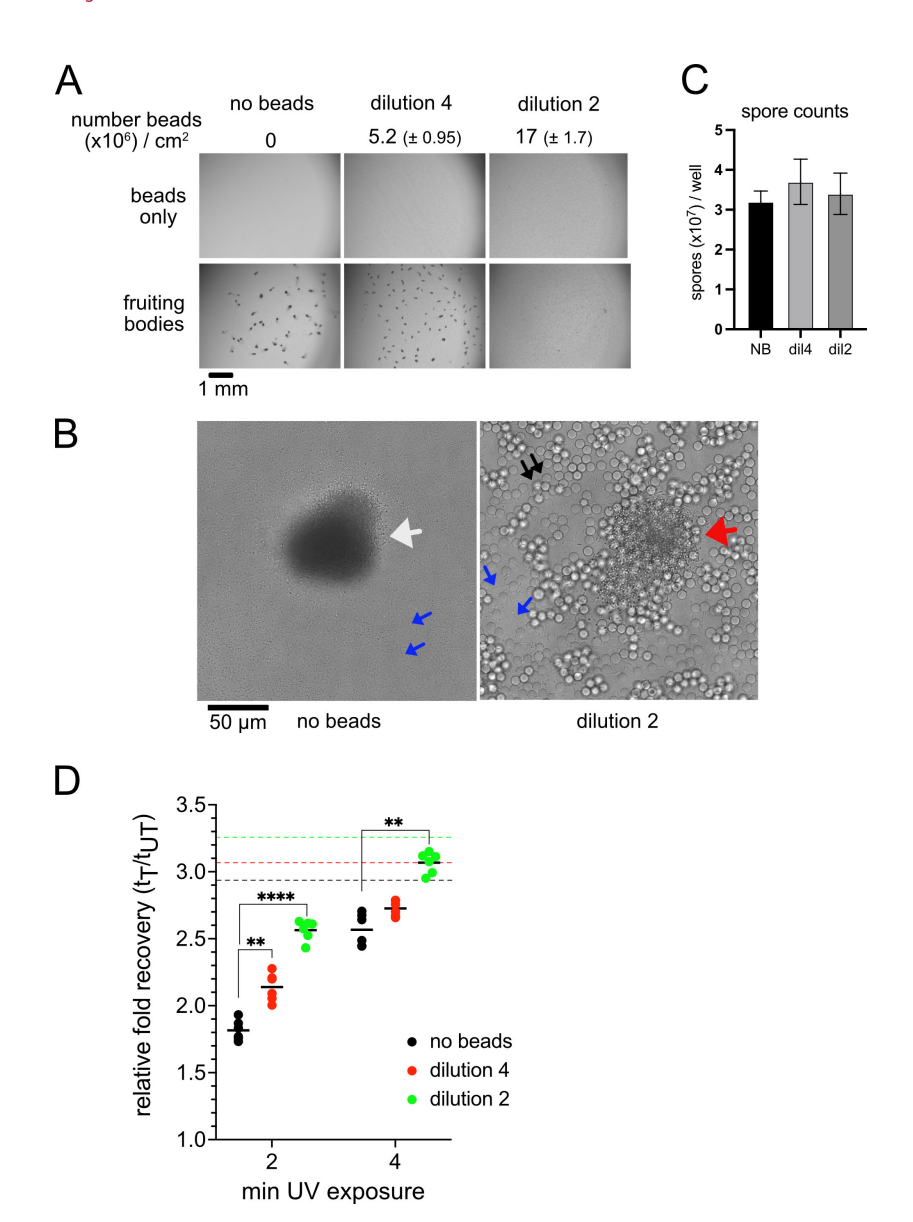


FIG 7 Production of small or microscopic fruiting bodies in the wild-type strain leads to significantly decreased recovery after UV exposure. (A) Fruiting bodies produced by the wild-type strain incubated in 48-well tissue plates for 120 hours without beads (no beads) or in the presence of two different concentrations of beads as indicated (bottom panels). Wells containing beads without cells are shown in the respective top panels. (B) Representative fruiting body details were captured by the production of fruiting bodies in confocal dishes with the corresponding bead density as indicated. The average fruiting body height of micro-fruiting bodies was determined as 20 \pm 10 μ m, n = 7. White arrow: fruiting body; blue arrows: peripheral rods; red arrow: micro-fruiting body; and black arrows: beads. (C) The number of heat- and sonication-resistant spores produced per well from fruiting bodies induced in the absence or presence of beads as indicated. (D) Relative fold recovery of normal (no beads)-, small (bead dilution 4)-, or microscopic (bead dilution 2)-fruiting bodies after 2 or 4 min of UV exposure. Data points are treated samples (t_T) normalized to the untreated sample (t_{UT}) . t_T and t_{UT} are the recovery times necessary for the treated and untreated cultures, respectively, to obtain an A_{550} of 0.2. Horizontal colored dashed lines represent the maximum observable relative recovery that could be detected in 72 hours. Data were obtained from two independent biological replicates, each containing triplicate samples. Mean is indicated by solid line. Statistical significance was determined by performing two-way ANOVA followed by Tukey's multiple comparison test (**P < 0.01 and ****P < 0.0001).

Exposure to desiccation suggested that the SF and wild-type vegetative mats were both highly susceptible to as little as 1 day of desiccation (Fig. 6B). However, while the SF mutant and wild-type free spores showed fairly similar recovery up to 4 days of desiccation, SF free spores thereafter exhibited significantly increased relative recovery times (Fig. 6B). These results suggest the spores released from SF fruiting bodies may have some defects in desiccation resistance compared to the spores released from wild-type fruiting bodies. Strikingly though, in contrast to the spores in the wild-type fruiting bodies, which required only approximately twofold longer relative recovery time after 32 days of desiccation, spores in the shallow fruiting bodies required at least a 3.8-fold relative recovery time after only 2 days of desiccation (Fig. 6B). Interestingly, the SF mutant fruiting bodies were even more susceptible to desiccation than their free spores, which recovered within our 72-hour window even after 32 days of desiccation (Fig. 6B). Examination of the appearance of dehydrated fruiting bodies in the wild type and SF mutant revealed that the SF mutant fruiting bodies appeared to lose opacity within 1 day of desiccation, which correlates with failure to recover (Fig. S6; Fig. 6B). In contrast, only the edges of the wild-type fruiting bodies become translucent, even after 32 days of desiccation (Fig. S6). By 2 days of desiccation, cracks occurred through the middle of the shallow fruiting mutant fruiting bodies and around the edges of wild-type fruiting bodies (data not shown and Fig. S6), suggesting the matrix was severely dehydrated and pulling away from the surface. We suggest that dehydration of the intact ECM may hinder spore germination, with the thin SF mutant dehydrating far more quickly than the wild-type taller fruiting body.

DISCUSSION

In this study, we examined the hypothesis that *M. xanthus* fruiting bodies protect the quiescent spores from environmental stresses. We demonstrated that spores inside wild-type fruiting bodies can tolerate significantly more UV exposure than the free spores (Fig. 3). In contrast, spores themselves are highly resistant to desiccation (Fig. 4). Fruiting bodies provide no additional protection up to ~1 week of desiccation and actually impeded recovery after extended desiccation (Fig. 4). The haystack structure and/or height of *M. xanthus* fruiting bodies is important, because shallow disorganized fruiting bodies do not provide additional protection from UV, and significantly interfere in recovery after desiccation (Fig. 6). These results suggest that *M. xanthus* fruiting body morphology may have been evolutionarily optimized to balance protection from UV and desiccation.

As part of this study, we developed a quantitative method to assess community recovery from insults rather than relying on the enumeration of colony-forming units arising after exposure to plating single cells/spores. *M. xanthus* favors community behavior in all aspects of its lifecycle, and communities may be slightly more tolerant to insults than individual cells because of resources that may be diminished if cells are separated [e.g., ECM components, co-operative repair or damage dilution mechanisms (48, 49), or phenotypic heterogeneity that is destroyed upon harvesting of the community (43)]. Furthermore, recovery of the community may be enhanced by group germination (50) or by the release of nutrients or eDNA from lysing cells that may promote growth and mutational repair, respectively (51). To avoid as much external manipulation of the community as possible, we, therefore, simply restored growth media to challenged communities and then used the time to recover to early exponential growth as a proxy for community resilience to insult. To compare the relative resistances of the cell states, we normalized the recovery times after insult to that of the respective untreated cell states.

M. xanthus spores isolated from fruiting bodies are well known to be more resistant to UV exposure than vegetative cells (29–31), which is at least partly due to the accumulation of a small, acid-soluble protein inside the spores (31). Previous assays suggested that spores released from 10-day-old fruiting bodies were up to 5.4 times more resistant to UV (15W germicidal lamp at 56 cm) than vegetative cells when assayed over the course

of 90 seconds (29). Consistently, in our assays, free spores were approximately twofold more resilient to 1 min of UV exposure than vegetative mats (Fig. 3), which may be comparable, given that our UV dose was likely much higher. Importantly, however, we demonstrate here that wild-type fruiting bodies were significantly more resistant to UV than free spores. Recovery of fruiting bodies after 1 min of UV exposure was similar to the untreated sample, and even after 8 min of UV exposure, it took on average ~2.4-fold longer than the untreated samples to recover. This type of UV and exposure level is biologically relevant. First, UV-B (280–320 nm) is considered the most biologically important source of UV, because it is not fully absorbed by the ozone layer and can cause direct damage to DNA via induction of pyrimidine dimers or production of free radicals that can damage other biological processes (52). Second, the dose is relevant; an average June day in Florida experiences 35 KJ/m² of UV-B (53). Fruiting bodies recovered from exposure to 0.08 KJ/m²/second for up to 8 min, corresponding to a 32.4 KJ/m² dose. We note that no recovery was observed in 72 hours of outgrowth after 16 min (64.8 KJ/m²) of UV exposure (data not shown), which is twice the Floridian daily dose.

We speculate that M. xanthus fruiting body morphology may be optimal to protect spores from environmental UV dosage. Mature wild-type fruiting bodies produced in our conditions are, on average, 77 \pm 14 μm in height (Fig. 5). For reference, UV-B penetrates 10–50 µm into the human epidermis (54), and spores are likely less penetrant than layers of skin. Therefore, it is likely that UV-B does not fully penetrate the interior of the fruiting body, and the ECM or outer layers of spores effectively shield the spores located in the interior. Consistent with this hypothesis, the shallow fruiting bodies produced by the SF mutant, with an average height that is at least threefold shorter than the wild type (Fig. 5), did not provide significant protection over the respective free spores (Fig. 6A). It is also possible that the fruiting body ECM, which consists of polysaccharides, proteins, eDNA, and vesicles (25-28), also contributes to protection from UV. For example, purified extracellular polysaccharides have been shown to protect from UV-B by scavenging reactive oxygen species produced during UV irradiation (55). The SF mutant does contain ECM because the shallow fruiting bodies are efficiently labeled by the lectin Concanavalin A [which binds to some of the ECM polysaccharides (28, 56), data not shown]. However, because SF spores are produced earlier during the developmental program than in the wild type (37), the total ECM may be reduced. The micro-fruiting bodies induced by the wild type upon increased substratum surface heterogeneity display a significant increase in relative recovery time after 2 or 4 min of UV exposure relative to the fruiting bodies produced on the homogenous surface (Fig. 7). Although the micro-fruiting bodies were a similar height to those produced by the shallow fruiting mutant, they were able to recover more efficiently after UV exposure. The presence of beads likely results in some shadowing of cells in the close vicinity that lowers the effective UV dosage of these samples relative to the no-bead control. Thus, it is possible that the actual UV sensitivity is comparable to that of the shallow fruiting bodies produced by the SF mutant. However, we cannot rule out that specific differences in the shape of the fruiting bodies, relative differences in ECM production, or specific resistance features of wild-type spores are important for the enhanced recovery of micro-fruiting bodies produced by the wild type vs the shallow fruiting bodies produced by the SF mutant. Regardless, the observation that heterogeneity in the surface can alter UV sensitivity is another important factor that needs to be considered in modeling how myxobacteria will respond to stresses in the environment.

Desiccation is a frequent stress experienced by environmental organisms, and extreme dehydration is lethal. Not only is water essential for metabolic activities, but it also prevents the aggregation of proteins and damage to membranes and DNA (57). *M. xanthus* spores exhibit two common protections against desiccation: reduced metabolic activity (58), which requires less water (59), and accumulation of trehalose (60, 61), a compatible solute that is thought to maintain protein solubility and stabilize membranes (62). In our assay, free spores released from either the wild type or SF mutant could recover reasonably efficiently after desiccation for at least 32 days (Fig. 6). Surprisingly, if

the spores were left in their native fruiting body state, recovery was slightly (wild type) or severely (SF mutant) hindered. One difference between these two states is that free spores lack the ECM; it is disrupted during the mild sonication to release the spores from the fruiting bodies and is removed when the free spores are pelleted. We suggest severe dehydration of the fruiting body ECM leads to a "glue" that is recalcitrant to rehydration, such that germination signals failed to reach the spores and/or partially germinated cells were unable to release themselves from the glue-like matrix. This severe dehydration likely only occurs where the matrix is thin: at the edges of the wild-type fruiting bodies but throughout the shallow fruiting bodies of the SF mutant. After desiccation, these areas image as translucent and accumulate cracks associated with water loss (Fig. S6). In contrast, the centers of the wild-type fruiting bodies remain opaque, and cracks do not transect the mound. Thus, while the *M. xanthus* fruiting body does not provide spores with additional protection from desiccation *per se*, we hypothesize that the wild-type haystack shape may limit excessive dehydration of the ECM.

We conclude that the M. xanthus fruiting bodies play an important role in protecting the spores from environmental insults. Perhaps this is necessary because myxospores are not very hardy; they are considerably more sensitive than endospores produced by Bacillus and Clostridium species (63). This study also revealed that M. xanthus fruiting bodies are not equally protective against all environmental stresses, suggesting they may have evolved as a middle ground providing some resistance to several distinct stresses. There are likely additional factors conferred by fruiting bodies that contribute to their net ecological advantage, such as enhancing spore maturation (17, 18). Our data hint that full desiccation resistance may be partially facilitated by maturation within fruiting bodies because (i) chemical-induced spores seem to display a slightly increased relative fold recovery compared to spores released from fruiting bodies (Fig. S5B vs Fig. 4), and (ii) SF mutant spores released from shallow fruiting bodies are less resistant to extended desiccation than those of the wild type (Fig. 6B), even though chemically induced spores from both strains share similar resistance (Fig. S5B). We are especially interested in the possibility that M. xanthus can tune its fruiting body morphology to distinct environmental conditions. The SF mutant we used in this study is a deletion of numerous signal systems that regulate the timing of development (34-36). Perhaps these signaling systems monitor the environment for signals, indicating rapid production of shallow fruiting body would be advantageous over haystack-shaped fruiting bodies. In an extreme example, M. xanthus can bypass fruiting bodies entirely to produce "free" spores in response to peptidoglycan damaging agents (64) or chemical signals from other microorganisms (65).

We suspect that the variety of fruiting body morphologies produced by other myxobacteria species is optimized to provide protection from stresses encountered in different niches. *M. xanthus* is among the few myxobacteria that produce fruiting bodies of a "globular soft mucous consistency" (12); most species produce either fruiting bodies of hardened slime or produce spores within a defined wall (sporangiole) (13, 14). It is likely that these fruiting bodies provide even more resistance to environmental insults, and it would be interesting to see if these species are enriched in more extreme environments.

ACKNOWLEDGMENTS

The authors gratefully acknowledge Bongsoo Lee for the construction of strains PH1054 and PH2036, and Gillian Leung for the construction of strain PH2037. We acknowledge past and present members of the Higgs lab for helpful discussions and/or critical reading of the manuscript.

This research was funded by a grant from the National Sciences Foundation IOS CAREER 1651921 (P.I.H.). The funders had no role in study design, data collection and interpretation, or the decision to submit the work for publication.

AUTHOR AFFILIATION

¹Department of Biological Sciences, Wayne State University, Detroit, Michigan, USA

AUTHOR ORCIDs

Penelope I. Higgs http://orcid.org/0000-0003-4726-3329

FUNDING

Funder	Grant(s)	Author(s)
National Science Foundation (NSF)	1651921	Dave Lall
		Maike M. Glaser
		Penelope I. Higgs

AUTHOR CONTRIBUTIONS

Dave Lall, Formal analysis, Investigation, Writing – original draft, Writing – review and editing | Maike M. Glaser, Investigation | Penelope I. Higgs, Conceptualization, Formal analysis, Funding acquisition, Writing – original draft, Writing – review and editing

ADDITIONAL FILES

The following material is available online.

Supplemental Material

Supplemental figures (AEM01660-24-s0001.docx). Figures S1 to S6.

REFERENCES

- Ma B, Stirling E, Liu Y, Zhao K, Zhou J, Singh BK, Tang C, Dahlgren RA, Xu J. 2021. Soil biogeochemical cycle couplings inferred from a function-taxon network. Res (Wash D C) 2021:7102769. https://doi.org/10.34133/2021/7102769
- Zakem EJ, Polz MF, Follows MJ. 2020. Redox-informed models of global biogeochemical cycles. Nat Commun 11:5680. https://doi.org/10.1038/ s41467-020-19454-w
- Cavicchioli R, Ripple WJ, Timmis KN, Azam F, Bakken LR, Baylis M, Behrenfeld MJ, Boetius A, Boyd PW, Classen AT, et al. 2019. Scientists' warning to humanity: microorganisms and climate change. Nat Rev Microbiol 17:569–586. https://doi.org/10.1038/s41579-019-0222-5
- Tiedje JM, Bruns MA, Casadevall A, Criddle CS, Eloe-Fadrosh E, Karl DM, Nguyen NK, Zhou J. 2022. Microbes and climate change: a research prospectus for the future. mBio 13:e0080022. https://doi.org/10.1128/ mbio.00800-22
- Morgan AD, MacLean RC, Hillesland KL, Velicer GJ. 2010. Comparative analysis of *Myxococcus* predation on soil bacteria. Appl Environ Microbiol 76:6920–6927. https://doi.org/10.1128/AEM.00414-10
- Nair RR, Velicer GJ. 2021. Predatory bacteria select for sustained prey diversity. Microorganisms 9:2079. https://doi.org/10.3390/microorganisms9102079
- Mayrhofer N, Velicer GJ, Schaal KA, Vasse M. 2021. Behavioral interactions between bacterivorous nematodes and predatory bacteria in a synthetic community. Microorganisms 9:1362. https://doi.org/10.3390/ microorganisms9071362
- Dai W, Wang N, Wang W, Ye X, Cui Z, Wang J, Yao D, Dong Y, Wang H. 2021. Community profile and drivers of predatory myxobacteria under different compost manures. Microorganisms 9:2193. https://doi.org/10. 3390/microorganisms9112193
- Petters S, Groß V, Söllinger A, Pichler M, Reinhard A, Bengtsson MM, Urich T. 2021. The soil microbial food web revisited: predatory myxobacteria as keystone taxa? ISME J 15:2665–2675. https://doi.org/10. 1038/s41396-021-00958-2

- Wang J, Wang J, Wu S, Zhang Z, Li Y. 2021. Global geographic diversity and distribution of the myxobacteria. Microbiol Spectr 9:e0001221. https://doi.org/10.1128/spectrum.00012-21
- Liu Y, Yao Q, Zhu H. 2019. Meta-16S rRNA gene phylogenetic reconstruction reveals the astonishing diversity of cosmopolitan myxobacteria. Microorganisms 7:551. https://doi.org/10.3390/microorganisms7110551
- Dawid W. 2000. Biology and global distribution of myxobacteria in soils. FEMS Microbiol Rev 24:403–427. https://doi.org/10.1111/j.1574-6976. 2000.tb00548.x
- Reichenbach H. 1993. Biology of the myxobacteria: ecology and taxonomy, p 13–62. In Dworkin M, Kaiser D (ed), Myxobacteria II. American Society for Microbiology.
- Reichenbach H. 1984. Myxobacteria: a most peculiar group of social prokaryotes, p 1–50. In Rosenberg E (ed), Myxobacteria, development and cell interactions. Springer-Verlag.
- Ward MJ, Zusman DR. 2000. Developmental aggregation and fruiting body formation in the gliding bacterium *Myxococcus xanthus*, p 243– 262. In Brun YV, Shimkets LJ (ed), Prokaryotic development. ASM Press, Washington DC.
- Kaiser D. 2001. Building a multicellular organism. Annu Rev Genet 35:103–123. https://doi.org/10.1146/annurev.genet.35.102401.090145
- Velicer GJ, Hillesland KL. 2008. Why cooperate? The ecology and evolution of the myxobacteria, p 17–40. In Whitworth DE (ed), Myxobacteria multicellularity and differentiation. ASM Press, Washington DC.
- Velicer GJ, Vos M. 2009. Sociobiology of the myxobacteria. Annu Rev Microbiol 63:599–623. https://doi.org/10.1146/annurev.micro.091208. 073158
- Zhang W, Wang Y, Lu H, Liu Q, Wang C, Hu W, Zhao K. 2020. Dynamics of solitary predation by Myxococcus xanthus on Escherichia coli observed at the single-cell level. Appl Environ Microbiol 86:e02286-19. https://doi. org/10.1128/AEM.02286-19
- Seef S, Herrou J, de Boissier P, My L, Brasseur G, Robert D, Jain R, Mercier R, Cascales E, Habermann BH, Mignot T. 2021. A Tad-like apparatus is

- required for contact-dependent prey killing in predatory social bacteria. Elife 10:e72409. https://doi.org/10.7554/eLife.72409
- Thiery S, Turowski P, Berleman JE, Kaimer C. 2022. The predatory soil bacterium *Myxococcus xanthus* combines a Tad- and an atypical type 3like protein secretion system to kill bacterial cells. Cell Rep 40:111340. https://doi.org/10.1016/j.celrep.2022.111340
- Rosenberg E, Keller KH, Dworkin M. 1977. Cell density-dependent growth of Myxococcus xanthus on casein. J Bacteriol 129:770–777. https://doi.org/10.1128/jb.129.2.770-777.1977
- 23. Thiery S, Kaimer C. 2020. The predation strategy of *Myxococcus xanthus*. Front Microbiol 11:2. https://doi.org/10.3389/fmicb.2020.00002
- Phillips KE, Akbar S, Stevens DC. 2022. Concepts and conjectures concerning predatory performance of myxobacteria. Front Microbiol 13:1031346. https://doi.org/10.3389/fmicb.2022.1031346
- Behmlander RM, Dworkin M. 1994. Biochemical and structural analyses of the extracellular matrix fibrils of *Myxococcus xanthus*. J Bacteriol 176:6295–6303. https://doi.org/10.1128/jb.176.20.6295-6303.1994
- Pathak DT, Wei X, Bucuvalas A, Haft DH, Gerloff DL, Wall D. 2012. Cell contact-dependent outer membrane exchange in myxobacteria: genetic determinants and mechanism. PLoS Genet 8:e1002626. https://doi.org/ 10.1371/journal.pgen.1002626
- 27. Hu W, Li L, Sharma S, Wang J, McHardy I, Lux R, Yang Z, He X, Gimzewski JK, Li Y, Shi W. 2012. DNA builds and strengthens the extracellular matrix in *Myxococcus xanthus* biofilms by interacting with exopolysaccharides. PLoS One 7:e51905. https://doi.org/10.1371/journal.pone.0051905
- Islam ST, Vergara Alvarez I, Saïdi F, Guiseppi A, Vinogradov E, Sharma G, Espinosa L, Morrone C, Brasseur G, Guillemot J-F, Benarouche A, Bridot J-L, Ravicoularamin G, Cagna A, Gauthier C, Singer M, Fierobe H-P, Mignot T, Mauriello EMF. 2020. Modulation of bacterial multicellularity via spatio-specific polysaccharide secretion. PLoS Biol 18:e3000728. https:// doi.org/10.1371/journal.pbio.3000728
- Sudo SZ, Dworkin M. 1969. Resistance of vegetative cells and microcysts of *Myxococcus xanthus*. J Bacteriol 98:883–887. https://doi.org/10.1128/ jb.98.3.883-887.1969
- Tengra FK, Dahl JL, Dutton D, Caberoy NB, Coyne L, Garza AG. 2006. CbgA, a protein involved in cortex formation and stress resistance in Myxococcus xanthus spores. J Bacteriol 188:8299–8302. https://doi.org/ 10.1128/JB.00578-06
- Dahl JL, Fordice D. 2011. Small acid-soluble proteins with intrinsic disorder are required for UV resistance in *Myxococcus xanthus* spores. J Bacteriol 193:3042–3048. https://doi.org/10.1128/JB.00293-11
- Galperin MY. 2013. Genome diversity of spore-forming firmicutes. Microbiol Spectr 1:TBS-0015-2012. https://doi.org/10.1128/microbiol-spectrum.TBS-0015-2012
- Campos JM, Zusman DR. 1975. Regulation of development in Myxococcus xanthus: effect of 3':5'-cyclic AMP, ADP, and nutrition. Proc Natl Acad Sci U S A 72:518–522. https://doi.org/10.1073/pnas.72.2.518
- Schramm A, Lee B, Higgs PI. 2012. Intra- and interprotein phosphorylation between two-hybrid histidine kinases controls Myxococcus xanthus developmental progression. J Biol Chem 287:25060–25072. https://doi.org/10.1074/jbc.M112.387241
- Jagadeesan S, Mann P, Schink CW, Higgs Pl. 2009. A novel "four-component" two-component signal transduction mechanism regulates developmental progression in *Myxococcus xanthus*. J Biol Chem 284:21435–21445. https://doi.org/10.1074/jbc.M109.033415
- Rasmussen AA, Søgaard-Andersen L. 2003. TodK, a putative histidine protein kinase, regulates timing of fruiting body morphogenesis in Myxococcus xanthus. J Bacteriol 185:5452–5464. https://doi.org/10.1128/ JB.185.18.5452-5464.2003
- Lee B, Higgs Pl. 2009. The role of negative regulators in coordination of the Myxococcus xanthus developmental program PhD Thesis, University of Marburg
- Müller F-D, Treuner-Lange A, Heider J, Huntley SM, Higgs Pl. 2010. Global transcriptome analysis of spore formation in *Myxococcus xanthus* reveals a locus necessary for cell differentiation. BMC Genomics 11:264. https://doi.org/10.1186/1471-2164-11-264
- Wood JL, Osman A, Wade SA. 2019. An efficient, cost-effective method for determining the growth rate of sulfate-reducing bacteria using spectrophotometry. MethodsX 6:2248–2257. https://doi.org/10.1016/j. mex.2019.09.036

- Lee B, Schramm A, Jagadeesan S, Higgs Pl. 2010. Two-component systems and regulation of developmental progression in *Myxococcus* xanthus. Methods Enzymol 471:253–278. https://doi.org/10.1016/S0076-6879(10)71014-4
- Dworkin M, Gibson SM. 1964. A system for studying microbial morphogenesis: rapid formation of microcysts in *Myxococcus xanthus*. Science 146:243–244. https://doi.org/10.1126/science.146.3641.243
- Higgs PI, MerlieJP. 2008. Myxococcus xanthus: cultivation, motility, and development, p 465–478. In Whitworth D (ed), Myxobacteria: multicellularity and differentiation. ASM Press.
- Lee B, Holkenbrink C, Treuner-Lange A, Higgs PI. 2012. Myxococcus xanthus developmental cell fate production: heterogeneous accumulation of developmental regulatory proteins and reexamination of the role of MazF in developmental lysis. J Bacteriol 194:3058–3068. https://doi.org/10.1128/JB.06756-11
- Higgs PI, Jagadeesan S, Mann P, Zusman DR. 2008. EspA, an orphan hybrid histidine protein kinase, regulates the timing of expression of key developmental proteins of *Myxococcus xanthus*. J Bacteriol 190:4416– 4426. https://doi.org/10.1128/JB.00265-08
- Sun H, Shi W. 2001. Genetic studies of mrp, a locus essential for cellular aggregation and sporulation of Myxococcus xanthus. J Bacteriol 183:4786–4795. https://doi.org/10.1128/JB.183.16.4786-4795.2001
- Ramos CH, Rodríguez-Sánchez E, Del Angel JAA, Arzola AV, Benítez M, Escalante AE, Franci A, Volpe G, Rivera-Yoshida N. 2021. The environment topography alters the way to multicellularity in *Myxococcus xanthus*. Sci Adv 7:eabh2278. https://doi.org/10.1126/sciadv.abh2278
- Tande BM, Pringle TA, Rutala WA, Gergen MF, Weber DJ. 2018. Understanding the effect of ultraviolet light intensity on disinfection performance through the use of ultraviolet measurements and simulation. Infect Control Hosp Epidemiol 39:1122–1124. https://doi. org/10.1017/ice.2018.144
- Dey A, Wall D. 2014. A genetic screen in Myxococcus xanthus identifies mutants that uncouple outer membrane exchange from a downstream cellular response. J Bacteriol 196:4324–4332. https://doi.org/10.1128/JB. 02217-14
- Vassallo CN, Wall D. 2016. Tissue repair in myxobacteria: a cooperative strategy to heal cellular damage. Bioessays 38:306–315. https://doi.org/ 10.1002/bies.201500132
- Pande S, Pérez Escriva P, Yu Y-T, Sauer U, Velicer GJ. 2020. Cooperation and cheating among germinating spores. Curr Biol 30:4745–4752. https://doi.org/10.1016/j.cub.2020.08.091
- Wang J, Hu W, Lux R, He X, Li Y, Shi W. 2011. Natural transformation of Myxococcus xanthus. J Bacteriol 193:2122–2132. https://doi.org/10.1128/ JB.00041-11
- Santos AL, Moreirinha C, Lopes D, Esteves AC, Henriques I, Almeida A, Domingues MRM, Delgadillo I, Correia A, Cunha A. 2013. Effects of UV radiation on the lipids and proteins of bacteria studied by mid-infrared spectroscopy. Environ Sci Technol 47:6306–6315. https://doi.org/10. 1021/es400660g
- Lee-Taylor J, Madronich S, Fischer C, Mayer B. 2010. A climatology of UV radiation, p 65S–65N. In UV radiation in global climate change: measurements, modeling and effects on ecosystems. Springer, Berlin, Heidelberg.
- Meinhardt M, Krebs R, Anders A, Heinrich U, Tronnier H. 2008. Wavelength-dependent penetration depths of ultraviolet radiation in human skin. J Biomed Opt 13:044030. https://doi.org/10.1117/1.2957970
- Peng S, Guo C, Wu S, Duan Z. 2022. Isolation, characterization and anti-UVB irradiation activity of an extracellular polysaccharide produced by Lacticaseibacillus rhamnosus VHPriobi O17. Heliyon 8:e11125. https://doi. org/10.1016/j.heliyon.2022.e11125
- Ducret A, Fleuchot B, Bergam P, Mignot T. 2013. Direct live imaging of cell-cell protein transfer by transient outer membrane fusion in Myxococcus xanthus. Elife 2:e00868. https://doi.org/10.7554/eLife.00868
- Aung K, Jiang Y, He SY. 2018. The role of water in plant-microbe interactions. Plant J 93:771–780. https://doi.org/10.1111/tpj.13795
- Watson BF, Dworkin M. 1968. Comparative intermediary metabolism of vegetative cells and microcysts of *Myxococcus xanthus*. J Bacteriol 96:1465–1473. https://doi.org/10.1128/jb.96.5.1465-1473.1968
- Rittershaus ESC, Baek S-H, Sassetti CM. 2013. The normalcy of dormancy: common themes in microbial quiescence. Cell Host Microbe 13:643–651. https://doi.org/10.1016/j.chom.2013.05.012

- McBride MJ, Zusman DR. 1989. Trehalose accumulation in vegetative cells and spores of *Myxococcus xanthus*. J Bacteriol 171:6383–6386. https://doi.org/10.1128/jb.171.11.6383-6386.1989
- Kimura Y, Kawasaki S, Tuchimoto R, Tanaka N. 2014. Trehalose biosynthesis in *Myxococcus xanthus* under osmotic stress and during spore formation. J Biochem 155:17–24. https://doi.org/10.1093/jb/ mvt091
- Potts M. 1994. Desiccation tolerance of prokaryotes. Microbiol Rev 58:755–805. https://doi.org/10.1128/mr.58.4.755-805.1994
- 63. Nicholson WL, Fajardo-Cavazos P, Rebeil R, Slieman TA, Riesenman PJ, Law JF, Xue Y. 2002. Bacterial endospores and their significance in stress
- resistance. Antonie Van Leeuwenhoek 81:27–32. https://doi.org/10. 1023/a:1020561122764
- O'Connor KA, Zusman DR. 1997. Starvation-independent sporulation in *Myxococcus xanthus* involves the pathway for beta-lactamase induction and provides a mechanism for competitive cell survival. Mol Microbiol 24:839–850. https://doi.org/10.1046/j.1365-2958.1997.3931757.x
- Marcos-Torres FJ, Volz C, Müller R. 2020. An ambruticin-sensing complex modulates *Myxococcus xanthus* development and mediates myxobacterial interspecies communication. Nat Commun 11:5563. https://doi.org/ 10.1038/s41467-020-19384-7